AERODYNAMIC ACTIVE VIBRATION ALLEVIATION FOR BUFFET EXCITED VERTICAL TAILS

Christian Breitsamter

Institute for Fluid Mechanics, Technische Universität München
Boltzmannstrasse 15, 85748 Garching, Germany
e-mail: chris@flm.mw.tum.de

ABSTRACT

The efficiency of an active auxiliary rudder system in alleviating fin buffeting is investigated based on extensive low–speed wind tunnel tests. A modern fighter aircraft model of 1/15–scale is used representing a single–fin configuration of canard–delta wing type. A specific vertical tail is fabricated featuring a digitally controlled auxiliary rudder providing harmonic oscillations. The vertical tail is instrumented to measure unsteady surface pressures, fin tip accelerations and auxiliary rudder moments. Open–loop tests show that the fin unsteady pressure field is feeded with energy at the frequencies of the auxiliary rudder motions. With increasing frequency and deflection angle the rms surface pressures are shifted to higher levels even at high incidences. Therefore, closed–loop operations may reduce buffet loads by approximately 18 percent. A nearly constant rudder moment over the angle–of–attack range investigated substantiates the effectiveness of the auxiliary rudder concept also at high–α. The active control system employs single–input single–output control laws to alleviate buffeting in the first fin bending and torsion mode, respectively. Controller efficiency and stability parameters are evaluated using dynamic system simulations. The studies demonstrate that with active control fin tip acceleration spectral density peaks at the frequencies of the first fin eigenmodes can be reduced by as much as 60 percent at angles of attack up to 31 deg.

NOMENCLATURE

A_{F_T}	Surface area of auxiliary rudder, $0.02941\ m^2$	Re_{l_μ}	Reynolds number, $U_\infty l_\mu/\nu$
		S_{c_p}	Pressure spectral density, $[1/Hz]$
Can.	Canard deflection angle, [°]	$S_{F_{\ddot{y}}}$	Normalized power spectral density of fin tip accelerations
c_M	Moment coefficient		
$c_p(t)$	Pressure coefficient, $(p(t)-p_\infty)/q_\infty$	s, s_F	Wing half span, Fin span, $[m]$
$\overline{c}_p$	Time–averaged pressure coefficient	s_{F_T}	Span of auxiliary rudder, $0.0656\ m$
c_p'	Fluctuation part of c_p	t	Time, $[s]$
$c_{p_{rms}}$	rms–value of c_p', $\sqrt{\overline{c_p'^2}}$	U_∞	Freestream velocity, $[m/s]$
$\hat{c}_p$	Amplitude spectrum of pressure coefficient, $\sqrt{2\ S_{c_p}\,\Delta k\,U_\infty/\,l_\mu}$	v'	Lateral velocity fluctuations, $[m/s]$
		v_{rms}	rms value of v', $\sqrt{\overline{v'^2}}$
f	Frequency, $[Hz]$	$\ddot{y}_F(t)$	Fin tip accelerations, $[m/s^2]$
g	Gravitational acceleration, $9.81\ m/s^2$	x_F, z_F	Fin coordinates, $[m]$
L.E.,	Wing leading– and trailing–edge flap	α	Aircraft angle of attack, [°]
Tr.E.	deflection, respectively, [°]	β	Aircraft angle of sideslip, [°]
l_μ	Wing mean aerodynamic chord, $[m]$	Λ, λ	Aspect ratio, taper ratio
K_p	Controller gain parameter, $[°/g]$	ν	Kinematic viscosity, $[m^2/s]$
k	Reduced frequency, $f\,l_\mu/U_\infty$	φ	Leading–edge sweep, [°]
M_{ζ_T}	Auxiliary rudder moment, $[Nm]$	Φ	Phase angle, [°]
p, p_∞	Pressure, ambient pressure, $[Pa]$	*Subscripts*	
q_∞	Freestream dynamic pressure, $[Pa]$	C, F, W, ζ_T	Canard, Fin, Wing, Aux. rud.

Paper presented at the RTO AVT Symposium on "Advanced Flow Management: Part A – Vortex Flows and High Angle of Attack for Military Vehicles", held in Loen, Norway, 7-11 May 2001, and published in RTO MP-069(I).

Report Documentation Page

Form Approved
OMB No. 0704-0188

1. REPORT DATE	2. REPORT TYPE	3. DATES COVERED
00 MAR 2003	**N/A**	**-**

4. TITLE AND SUBTITLE	5a. CONTRACT NUMBER
Aerodynamic Active Vibration Alleviation for Buffet Excited Vertical Tails	5b. GRANT NUMBER
	5c. PROGRAM ELEMENT NUMBER
6. AUTHOR(S)	5d. PROJECT NUMBER
	5e. TASK NUMBER
	5f. WORK UNIT NUMBER
7. PERFORMING ORGANIZATION NAME(S) AND ADDRESS(ES) **NATO Research and Technology Organisation BP 25, 7 Rue Ancelle, F-92201 Neuilly-Sue-Seine Cedex, France**	8. PERFORMING ORGANIZATION REPORT NUMBER
9. SPONSORING/MONITORING AGENCY NAME(S) AND ADDRESS(ES)	10. SPONSOR/MONITOR'S ACRONYM(S)
	11. SPONSOR/MONITOR'S REPORT NUMBER(S)

12. DISTRIBUTION/AVAILABILITY STATEMENT
Approved for public release, distribution unlimited

13. SUPPLEMENTARY NOTES
Also see: ADM001490, Presented at RTO Applied Vehicle Technology Panel (AVT) Symposium held inLeon, Norway on 7-11 May 2001, The original document contains color images.

14. ABSTRACT

15. SUBJECT TERMS

16. SECURITY CLASSIFICATION OF:			17. LIMITATION OF ABSTRACT	18. NUMBER OF PAGES	19a. NAME OF RESPONSIBLE PERSON
a. REPORT	b. ABSTRACT	c. THIS PAGE			
unclassified	**unclassified**	**unclassified**	**UU**	**14**	

1 INTRODUCTION

Modern fighter aircraft are subject to high angle of attack manuevers extending the flight envelop to the stall and poststall regime.[1] Slender wing geometries, e.g. delta wing planforms, strakes, and leading–edge extensions (LEX), respectively, are used to generate strong large–scale vortices along the leading–edges. They improve significantly the high–α performance because of additional lift and an increase in maximum angle of attack.[2] At high angle of attack, however, the large–scale vortices burst already over the wing planform. The transition from stable to unstable core flow, evident by the rapid change in the axial velocity profiles from jet–type to wake–type, leads to an extremely high turbulence intensity peak at the breakdown position and an increased turbulence level downstream.[3] Hence, the buffet excitation level increases strongly above a certain α, and fin normal force spectra are characterized by narrow–band peaked distributions, Fig. 1. Such unsteady aerodynamic loads often excite the vertical tail structure in its natural frequencies resulting in increased fatigue loads, reduced service life and raised maintenance costs.[4]

The fin buffeting problem plagues twin–fin configurations (F–15, F/A–18, F–22), but single–fin aircraft are also affected.[5–8] Therefore, comprehensive research programs have been undertaken aimed at understanding the buffet loads and reducing the structural response. The related vortical flow features are carefully analyzed using wind tunnel tests on small–scale and full–scale models,[3–7] supplemented by flight tests,[7,8] and detailed numerical flow simulations.[9] Further, buffet prediction methods have been developed to identify buffet loads on various configurations.[10,11]

To improve the knowledge on the flow physics associated with fin buffeting, extensive experiments on the low–speed fin flow environment of a modern fighter aircraft model have been conducted at the Institute for Fluid Mechanics (FLM) of the Technische Universität München (TUM).[3,12] The studies focus on the turbulent flow structure well defined by the spatial and temporal characteristics of the unsteady flow velocities. It was found that the flow downstream of bursting is subject to a helical mode instability. The quasi–periodic velocity fluctuations associated with the most unstable normal mode of the mean axial velocity profile of the burst vortex core evoke coherent unsteady surface pressures (buffet).[11] Downstream of bursting maximum turbulence intensities are concentrated on a limited radial range related to the points of inflection in the radial profiles of the retarded axial core velocity. The flowfield surveys show that with increasing incidence the burst vortex cores grow significantly moving inboard and upward. Consequently, a center–line fin may also encounter high turbulence levels in the high–α

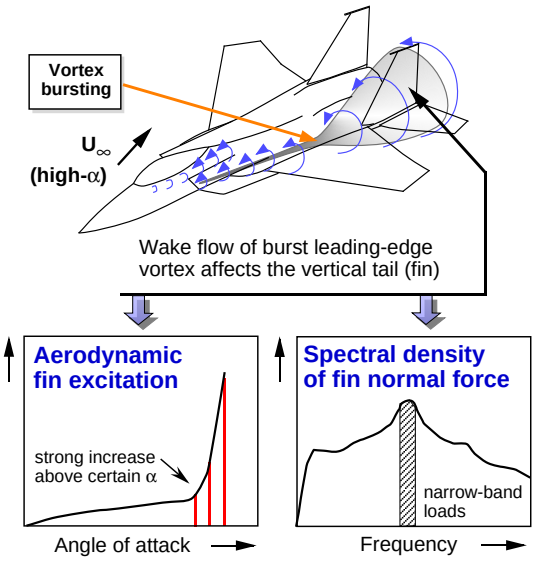

Fig. 1: Fin buffet flow characteristics.

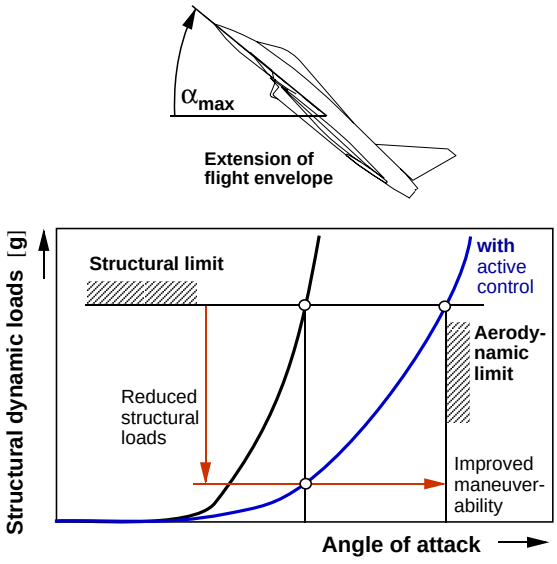

Fig. 2: Increase in performance by active buffet load alleviation.

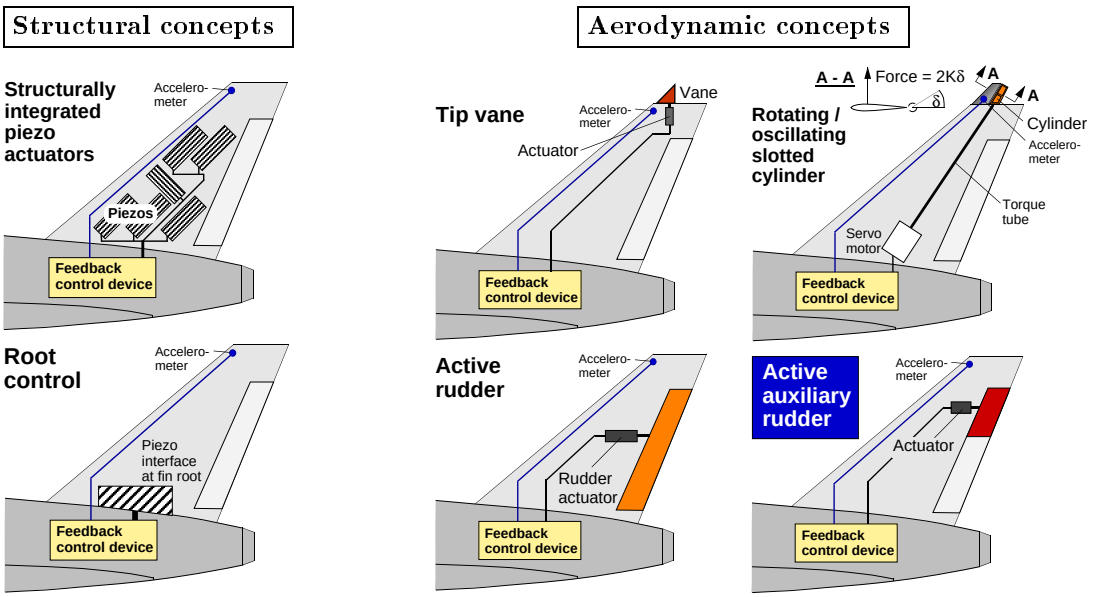

Fig. 3: System concepts for active buffet load alleviation.

regime.[12] Further, the turbulence intensities in the fin region may increase markedly for some sideslip reaching levels typically obtained at twin–fin stations where the fin is directly enveloped by the breakdown flow.[13]

The buffet loads do not only decrease the fatigue life of the airframe, but may, in turn, limit the angle–of–attack envelope of the aircraft. To counter the fin buffeting problem several methods have been suggested. They deal with alterations of the fin structural properties like stiffness and damping,[14] aerodynamic modifications for a passive or active control of vortex trajectories to avoid a direct impact of the burst vortical flow on the fin[5,7] and methods of active vibration control.[15,16] With active control the structural dynamic loads are reduced aimed not only to increase the service live but also to improve the maneuverability extending the flight envelope to higher angles of attack, Fig. 2. For active vibration alleviation various actuators have been discussed and tested involving both structural and aerodynamic concepts,[15–19] Fig. 3. The structural methods focus mainly on surface integrated piezo actuators or on a piezo interface between fin and fuselage structure.[16–19] In the aerodyamic field, a tip vane, a rotating or oscillating slotted cylinder mounted at the fin tip and an active rudder are studied.[15,16,18] Considering a real aircraft, the moving vane or slotted cylinder may not produce forces large enough to damp effectively the enforced vibrations. The rudder may work more efficiently but its mass hampers high frequency operations restricting the damping of structural vibrations usually to the first fin bending mode.[16] In addition, aircraft handling qualities could be affected. Therefore, an active auxiliary rudder is proposed realized by deviding the standard rudder into two parts where only the upper part is used for adaptive vibration control.

The experiments presented herein concentrate on the efficiency of the auxiliary rudder concept which is tested the first time on an EF–2000 wind tunnel model.[20] Here, mainly results for symmetric freestream are discussed whereas investigations for sideslip conditions are reported in Ref. 21.

2 EXPERIMENTAL SET–UP

2.1 Model and Facility

The experiments are conducted on a detailed rigid steel model of a modern fighter aircraft of canard–delta wing type (EF–2000 type), Fig. 4. The model consists of nose section, front fuselage with rotatable canards and a single place canopy, center fuselage with delta wing section and a through–flow double air intake underneath, and rear fuselage including nozzle section and

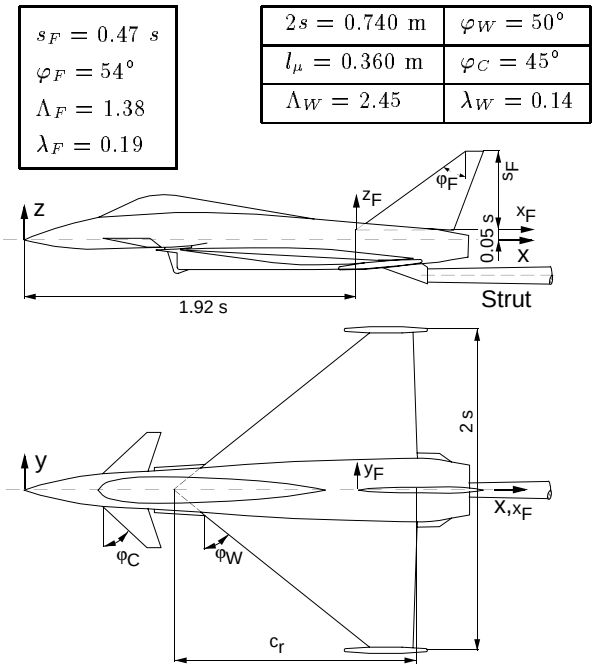

Fig. 4: Geometry of EF–2000 wind tunnel model.

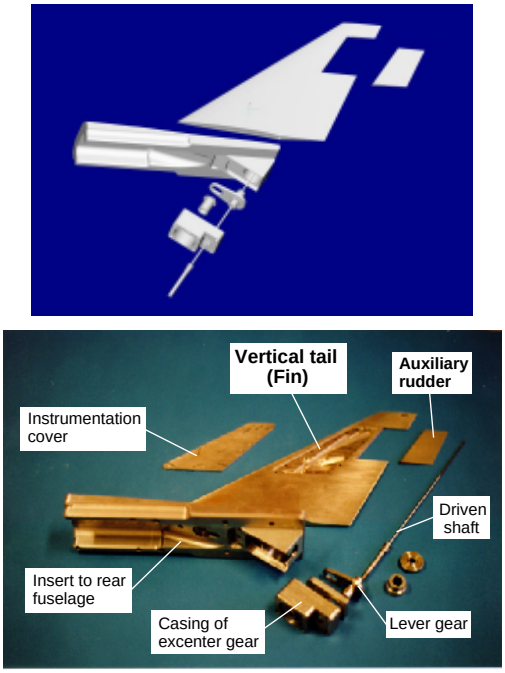

Fig. 5: CAD model and fabricated parts of fin section including active auxiliary rudder.

the vertical tail (fin). For the present investigations, a completely new fin section has been constructed fitted with an actively controlled auxiliary rudder. The computer–aided design (CAD) model and main assembly parts are shown in Fig. 5.

The fabricated parts include the fin with an instrumentation cover, the active auxiliary rudder, the body insert to fasten the fin to the rear fuselage and the driving components. The auxiliary rudder is commanded via an excenter gear by a computer–controlled servo motor providing har-

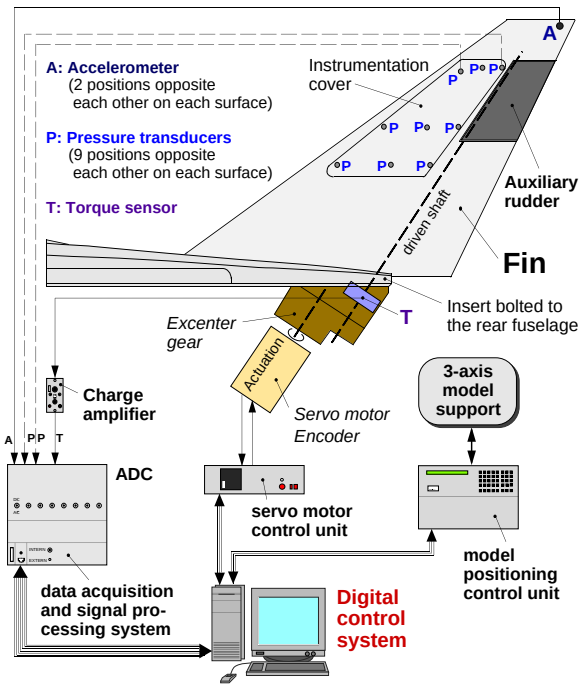

Fig. 6: Integrated measurement and control system for active fin buffet load alleviation.

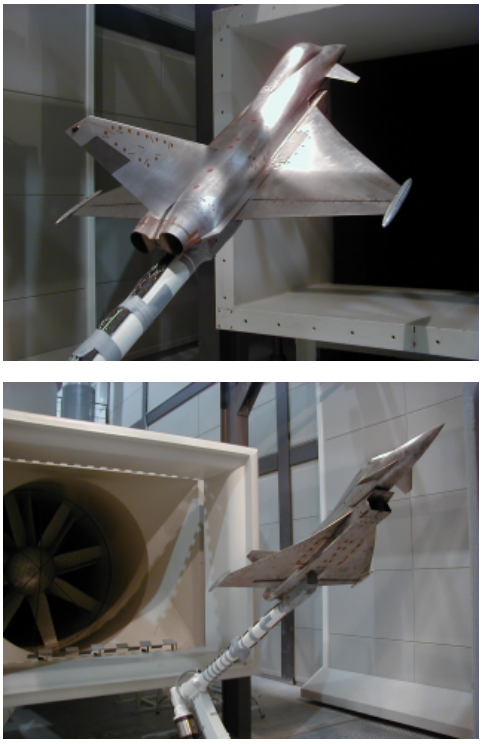

Fig. 7: Views of 1/15–scale EF–2000 model mounted in test section of FLM low speed wind tunnel B.

monic (sinusoidal) motions, Fig. 6. The oscillation frequency f_{ζ_T} can be adjusted digitally while the maximum rudder deflection angle is fixed mechanically to $\zeta_{T_{max}} = 1°, 3°, 5°$. The mass of the auxiliary rudder is only 0.015 kg to reduce inertia forces at a maximum oscillation frequency of 120 Hz. The fin is instrumented with 2 tip accelerometers, 18 differential unsteady pressure transducers at 9 positions directly opposite each other on each surface and a torque moment transducer at the driven rudder shaft (Fig. 6).
The investigations have been carried out in the Göttingen type low–speed wind tunnel B of the Institute for Fluid Mechanics of the Technische Universität München. The open test section is 1.2 m in height and 1.55 m in width and 2.8 m long. Maximum usable velocity is 60 m/s with a turbulence level less than 0.4%. The EF–2000 model is sting mounted on its lower surface by a computer–controlled three–axis model support, Fig. 7.

2.2 Test Conditions

Since active control of buffet–induced vibrations is the primary focus the first fin eigenmodes are of particular interest. At wind–off the first bending mode of the fin model is around 145 Hz and the first torsion mode is around 387 Hz. The structural damping is about 4.4%, whereas the aerodynamic damping is $3.2\% \div 4.8\%$ for $\alpha = 25° \div 31.2°$.
For buffet, the reduced frequency k with

$$k = \frac{f\, l_\mu}{U_\infty} = \frac{f_M\, l_{\mu_M}}{U_{\infty_M}} \qquad \text{M: Model} \tag{1}$$

is the basic similarity parameter in determining test conditions. The frequency ratio between the considered structural modes of the actual aircraft and the model is 1/8. The model scale is 1/15. With respect to low–speed, high angle–of–attack maneuvers the tests are made at a freestream reference velocity of $U_\infty = 40\ m/s$ corresponding to a Reynolds number of $Re_{l_\mu} = 0.97 \times 10^6$ based on the wing mean aerodynamic chord. The angle of attack is varied in the range of $0° \leq \alpha \leq 31.2°$ at sideslip angles of $\beta = 0°$, and 5°. The results shown herein concentrates mainly on $\beta = 0°$. Turbulent boundary layers are present at wing and control surfaces known from previous experiments.[3]
Using a multi–channel data acquisition system, output voltages of unsteady surface pressure transducers, fin tip accelerometers and the rudder moment sensor are amplified for optimal signal levels, low–pass filtered at 256 Hz and 1000 Hz, respectively, and simultaneously sampled and digitized with 14–bit precision. The sampling rate for each channel is set to 2000 Hz and the sampling interval is 30 s. The data acquisition parameters are based on preliminary tests to cover all significant flow phenomena as well as on statistical accuracies of 1%, and 2.5% for the rms values and spectral densities, respectively.[3,20]

3 BUFFET CHARACTERISTICS AND STRUCTURAL RESPONSE

3.1 Buffet Flowfield

Extensive studies on the vortical flowfields associated with fin buffeting have been conducted on generic models as well as on a modern fighter aircraft model.[3,11–13] The impact of the flowfield on the fin structure can be characterized by the lateral rms velocities surveyed carefully within the fin region. Summarizing, the rms values for different vertical fin stations are shown as function of angle of attack in Fig. 8a. The magnitude of the rms values in the midsection depends on the development of the vortical flow structure. This is depicted by the schematics of Fig. 8a which are based on the rms velocity patterns in planes normal to the fin surface, Figs. 8b-d. At moderate angles of attack the area of the center–line fin is only little affected by the highly turbulent flow regions attributed to the burst wing leading–edge vortices (WLVs) and canard leading–edge vortices (CLVs) and trailing–edge vortices (CTVs), Fig. 8b. Above $\alpha = 25°$, the lateral turbulence intensities in the fin region increase significantly with increasing angle of

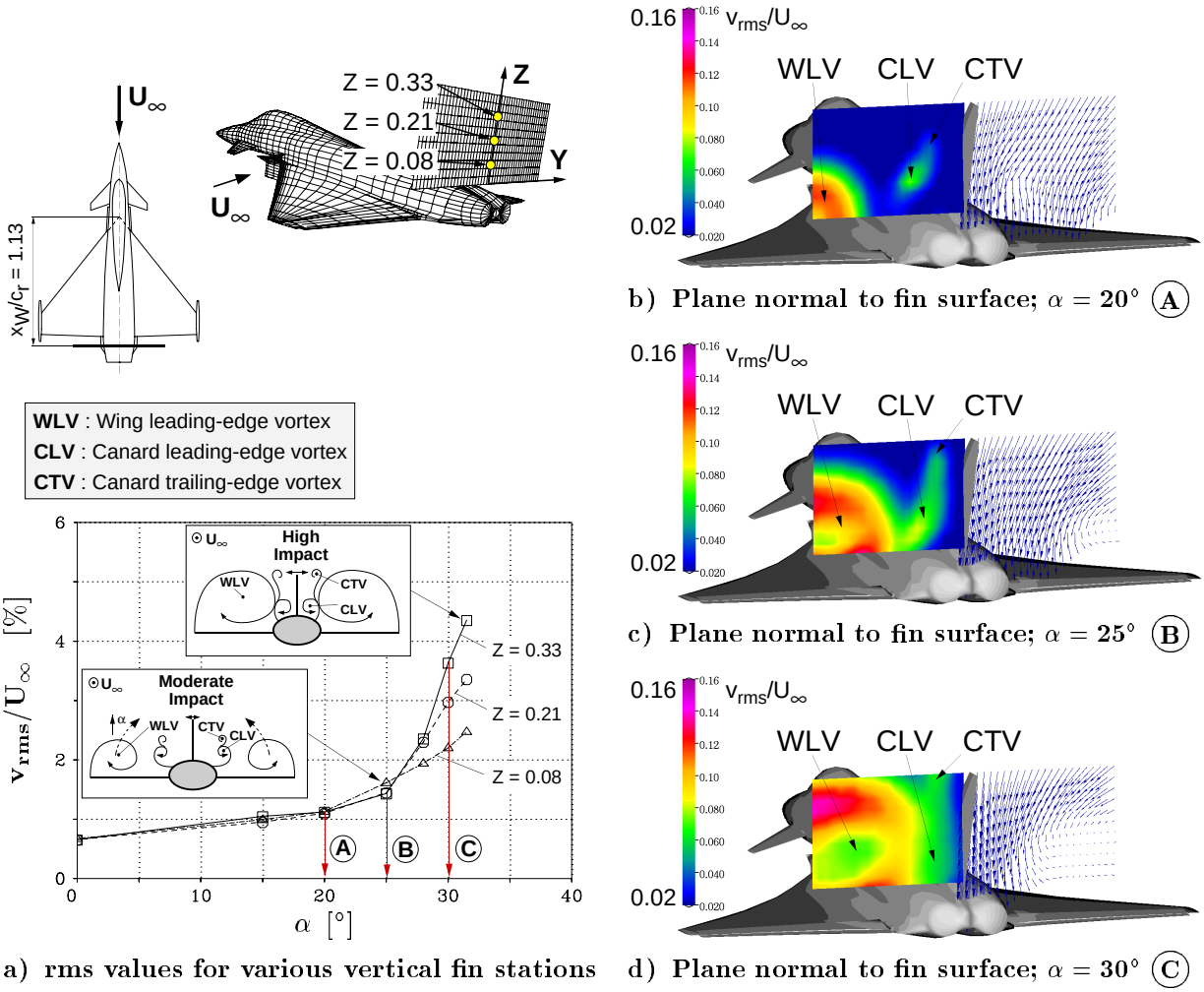

a) rms values for various vertical fin stations

b) Plane normal to fin surface; $\alpha = 20°$ (A)

c) Plane normal to fin surface; $\alpha = 25°$ (B)

d) Plane normal to fin surface; $\alpha = 30°$ (C)

Fig. 8: Lateral rms velocity v_{rms}/U_∞ and cross–flow velocity patterns measured in the fin region for various angles of attack; $U_\infty = 40$ m/s, $Re_{l_\mu} = 0.97 \times 10^6$, $\beta = 0°$, Refs. 11, 12.

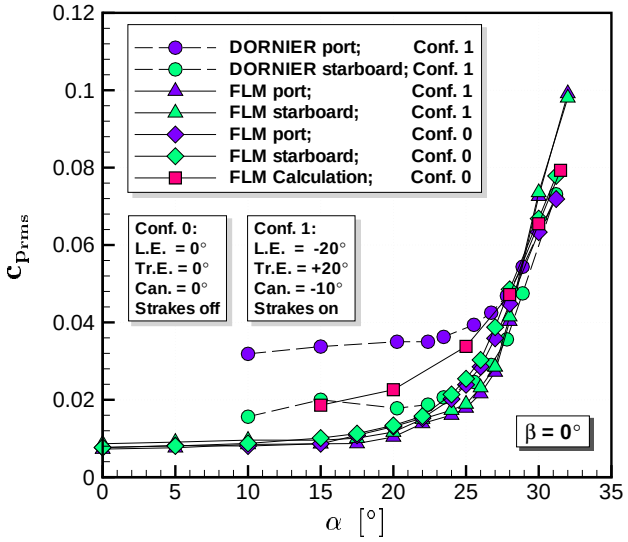

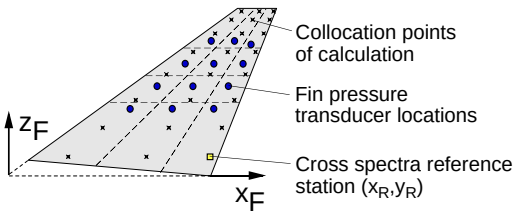

DORNIER: **12** pressure transducers at stations opposite each other on each surface

FLM: **9** pressure transducers at stations opposite each other on each surface

Calculation: **3 × 8** measurement/collocation points

Fig. 9: Measured and calculated fin buffet pressures as function of angle of attack; DORNIER: Ma = 0.5, $Re_{l_\mu} = 3.01 \times 10^6$, Ref. 3; FLM & Calculation: Ma = 0.12, $Re_{l_\mu} = 0.97 \times 10^6$.

attack as the burst WLVs expand and move upward and inboard thus approaching the mid section, Fig. 8c. The CLVs and CTVs are also pushed to the mid section because of a merging with the WLVs. In particular, the fin flow is influenced by induction effects arising from the expanding wing leading–edge vortex sheets which are the loci of maximum turbulence intensities, Fig. 8d. The interaction between WLVs and canard vortices (CLVs and CTVs) leads to local rms maxima within the fin area.[11]

3.2 Buffet Pressures

The corresponding surface pressure fluctuations defining the buffet situation are averaged for each side of the fin and plotted together as function of angle of attack, Fig. 9. Surface panels are used for averaging $c_{p_{rms}}$ (Fig. 9) assuming that the rms pressures are constant throughout the panels. The buffet pressures increase severely above $\alpha = 25°$ reflecting the rise in the lateral rms velocities. The results are taken from unsteady pressure measurements on different 1/15–scale models with different configurational details (DORNIER 1989, Ref. 3; FLM 1999, Ref. 20) as well as from pressure calculations based on the measured turbulent flowfields.[12] The data obtained show an excellent agreement over the considered angle–of–attack range.
For further analysis, buffet and buffeting are quantified by nondimensional spectral functions. The amplitude spectra of the buffet pressures show that turbulent energy is channeled into a narrow band, Fig. 10. This energy concentration is detected the first time at $\alpha \approx 22°$ because the helical mode instability of the burst WLVs starts to affect the fin pressure field. From $\alpha = 24°$ to $\alpha = 31.2°$ the narrow–band amplitudes increase while the dominant reduced frequencies k_{dom} are shifted to lower values. This frequency shift is caused by an increase in the wave length of the helical mode instability when raising the angle of attack.

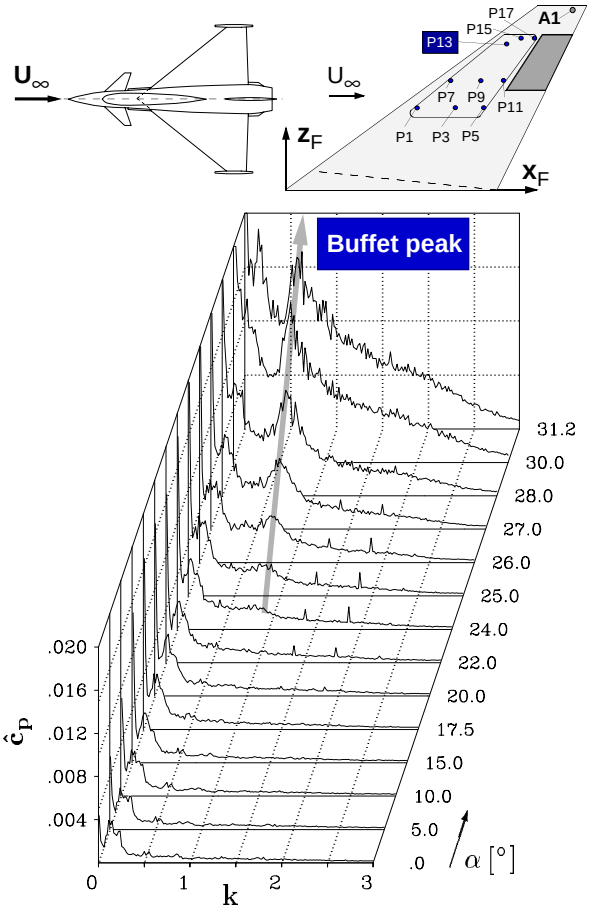

Fig. 10: Buffet pressure spectra $\hat{c}_p$ at station P13 for all angles of attack tested; $U_\infty = 40$ m/s, $Re_{l_\mu} = 0.97 \times 10^6$, $\beta = 0°$.

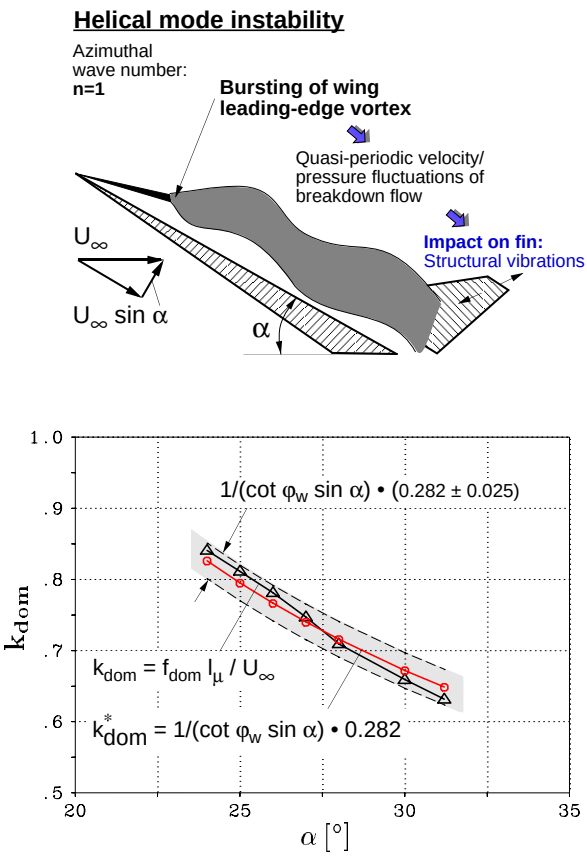

Fig. 11: Dominant reduced buffet frequency k_{dom} as function of angle of attack obtained from fin pressure spectra of station P13.

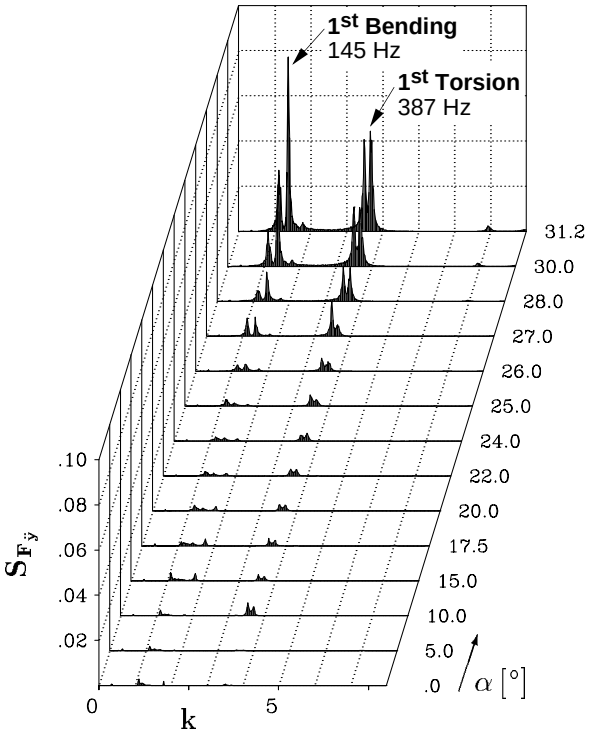

Fig. 12: PSDs of fin tip accelerations S_{F_y} for all angles of attack tested; $U_\infty = 40$ m/s, $Re_{l_\mu} = 0.97 \times 10^6$, $\beta = 0°$.

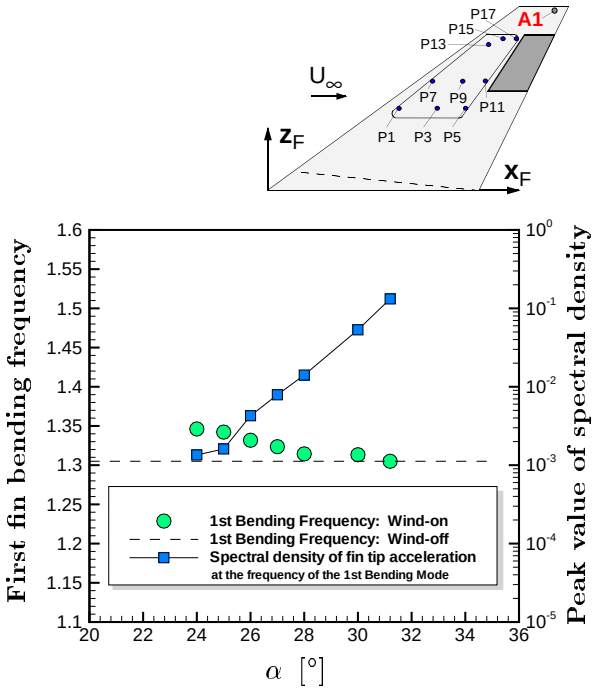

Fig. 13: First fin bending frequency and assigned PSD peak values as function of angle of attack.

As demonstrated in Fig. 11, a scaling with the sinus of α and the local semi–span $x \cdot \cot \varphi_W$ gives an approximately constant value of

$$k_{dom} \sin \alpha \cot \varphi_W \approx 0.282 \pm 0.025 . \quad (2)$$

The relationship of Eq. (2) leads to a design value for vortex burst dominant frequencies due to the helical mode instability of the breakdown flow including variations in angle of attack and wing sweep. These findings hold also for other experimental data.[5–7,10]

3.3 Buffeting

The pressure distributions discussed (Figs. 9–11) create the buffeting, or structural response to the buffet, typically quantified by power spectral densities (PSDs) of the fin tip accelerations, Fig. 12. The resulting fin buffeting consists mainly of a response in the first bending and torsion mode. At high–α, the dominant buffet frequency comes close to a value half of the bending eigenfrequency which is then strongly excited whereas the first torsion mode with a multiple higher eigenfrequency is less excited. Analyzing the spectra a gradual shift in the frequency of the first bending mode with angle of attack is found while the logarithmic growth of the amplitude values is nearly linear, Fig. 13. This shift in frequency may be seen as increases in aerodynamic damping regarding the fin as a single degree–of–freedom system excited by the large narrow–band perturbations of the breakdown flow.

4 OPEN–LOOP TESTS AND SYSTEM IDENTIFICATION

4.1 Passively and Actively Controlled Rudder

Open–loop tests are performed driving the auxiliary rudder harmonically (sinusoidally) at various frequencies f_{ζ_T} with maximum deflection angles $\zeta_{T_{max}} = 1°$, 3°, and 5°. For the oscillating rudder, the rms pressures are shifted to higher levels in comparison to the results for the symmetrically fixed or stationary deflected rudder.[20,21] The $c_{p_{rms}}$–curves show that the induced un-

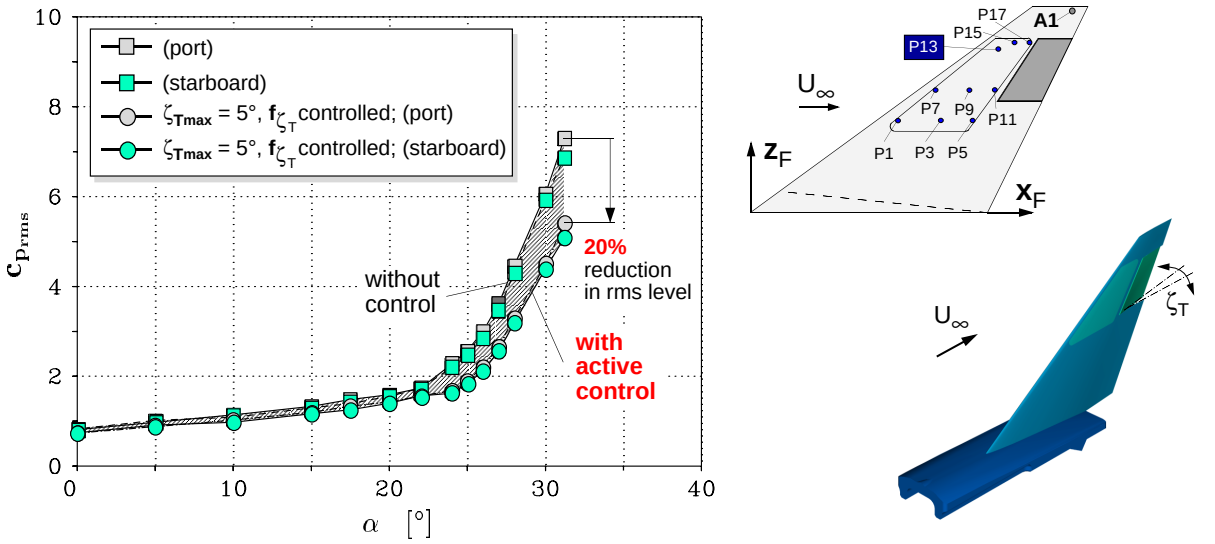

Fig. 14 Comparison of rms pressures $c_{p_{rms}}$ (averaged for each side of the fin) without and with auxiliary rudder control; $\zeta_{T_{max}} = 5°$, $U_\infty = 40$ m/s, $Re_{l_\mu} = 0.97 \times 10^6$, $\beta = 0°$.

steady pressures increase with increasing rudder frequency and still more with increasing rudder deflection angle over the whole angle–of–attack range tested. Closing the loop, the commanded auxiliary rudder may modify the buffet loads themselves with a potentiality to reduced buffet rms pressures by as much as 18% to 20%, Fig. 14.

The corresponding pressure spectra are characterized by narrow–band peaked distributions attributed to the helical mode instability of the breakdown flow, Fig. 15, as known already from the non–oscillating case (Fig. 10). However, a spike at the value of the auxiliary rudder frequency indicates that at this frequency the fluctuating pressure field is feeded with energy. As the peak amplitude remains nearly constant for all angles of attack regarded active rudder control may effectively alleviate the frequency dependent buffet loads.

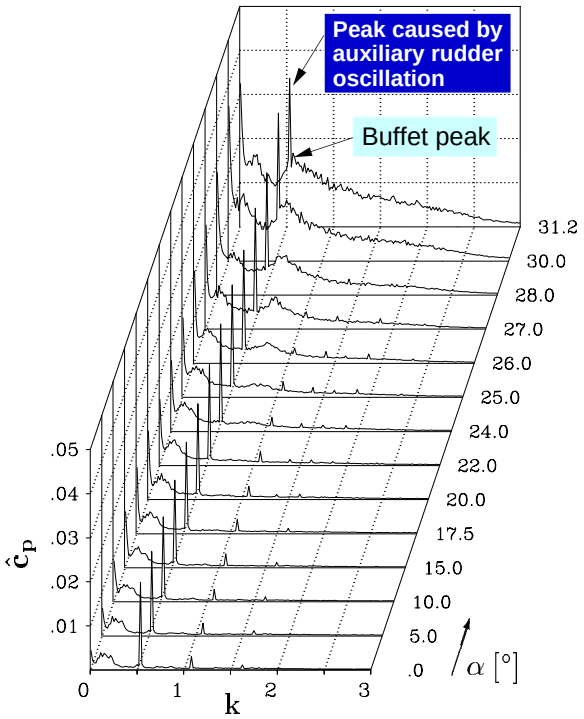

Fig. 15: Amplitude spectra of fin pressure fluctuations $\hat{c}_p$ at station P13 for all angles of attack tested at $k_{\zeta_T} = 0.540$ and $\zeta_{T_{max}} = 3°$; $U_\infty = 40$ m/s, $Re_{l_\mu} = 0.97 \times 10^6$, $\beta = 0°$.

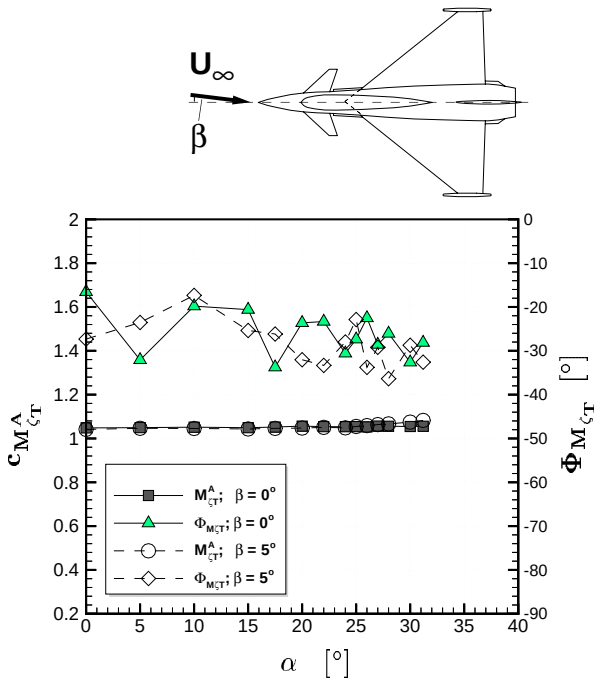

Fig. 16: Amplitude $c_{M^A_{\zeta_T}}$ and phase angle $\Phi_{M_{\zeta_T}}$ of the auxiliary rudder moment coefficient at $k_{\zeta_T} = 0.540$ and $\zeta_{T_{max}} = 3°$ as function of angle of attack; $\beta = 0°$, $5°$.

Further, the auxiliary rudder moment is analyzed representing an integral quantity, Fig. 16. The moment coefficient is calculated using dynamic freestream pressure q_∞ and the surface area A_{F_T} and span s_{F_T} of the auxiliary rudder.

$$c_{M_{\zeta_T}} = M_{\zeta_T}/(q_\infty A_{F_T} s_{F_T}) \quad (3)$$

The amplitude values of the first harmonic illustrate that there is no drop of the rudder moment at higher angles of attack while the phase angle varies between $-18°$ and $-36°$. The characteristic of an approximately constant rudder moment at all incidences demonstrates again that the auxiliary rudder work efficiently also in the high–α regime.

4.2 Open–Loop Frequency Response Function

The open–loop frequency response functions of the fin are calculated using the fourier–transformed discrete time series of auxiliary rudder deflection angles and fin tip accelerations. The frequency response functions are obtained for wind–off and wind–on conditions for several angles of attack, Fig. 17. To concentrate on the first fin bending mode around 145 Hz, the rudder frequency is commanded with a linear frequency sweep of $k = 0 \div 0.81$ (90 Hz) at $\zeta_{T_{max}} = 1°, 3°, 5°$. Consequently, the amplitude of the transfer function exhibits a peak value at the frequency of the first fin bending mode while the phase angle varies between ± 180 degree. (Note that fin tip accelerations related to the first bending mode become a maximum when the auxiliary rudder is driven at a frequency value half the value of the fin bending eigenfrequency.)

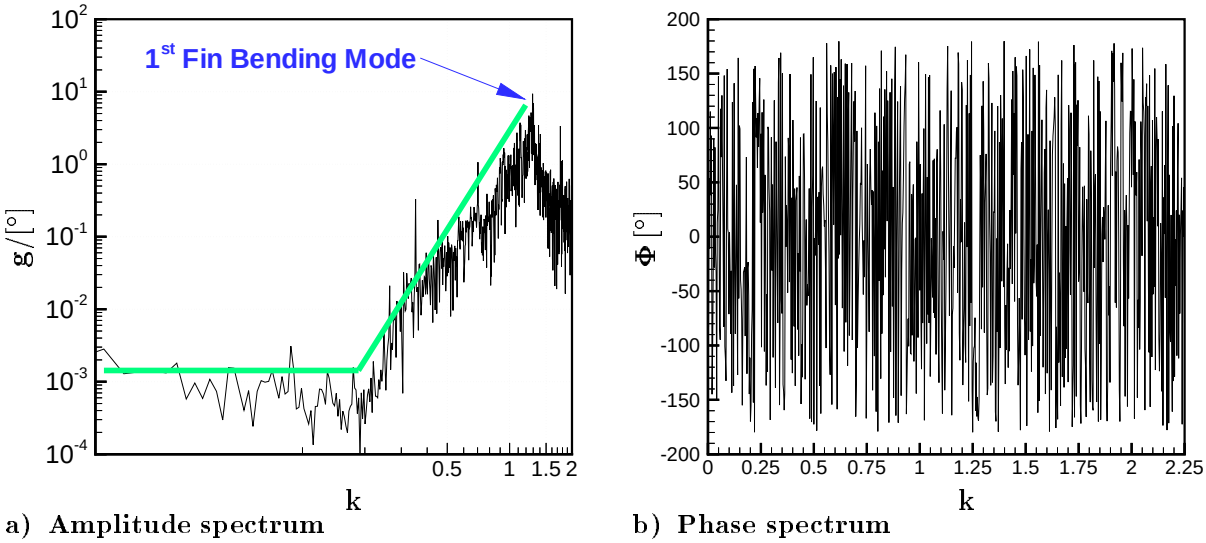

a) Amplitude spectrum b) Phase spectrum

Fig. 17: Open–Loop frequency response function of fin tip accelerations vs. commanded auxiliary rudder oscillations for a frequency sweep of k = 0 ÷ 0.81 at wind–on and $\alpha = 0°$.

5 ACTIVE BUFFETING ALLEVIATION

5.1 Control Law Design

The open–loop frequency response functions between the commanded rudder deflection angle and the fin tip acceleration are the input–output relationships of the forward loop of the active control system. As shown in Fig. 18, the buffet induced vibrations contribute to the response (output) of the fin, i.e. accelerations in this case. Hence, for a detailed controller design, the open–loop frequency response functions have to be determined for wind–off and wind–on conditions at various α since the buffet level increases with increasing incidence.

The active control system consists of an analog–to–digital (A/D) converter, a digital controller in which the control law is implemented, and a digital–to–analog (D/A) converter connected to amplifier, filter elements and encoder operating the servo motor as rudder actuator, Fig. 18a. Using the measured open–loop frequency response functions, control laws are designed with re-

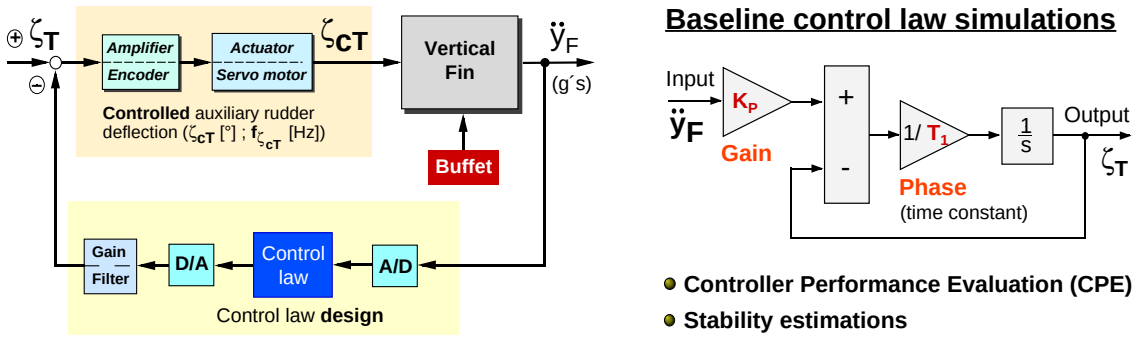

a) Control circuit b) Control law schematic

Fig. 18: Schematic of active control system.

spect to frequency domain compensation methods.[22] Single–input single–output relationships are employed with the tip accelerometers as sensors to alleviate the response in the first fin bending and torsion mode, respectively. The commanded rudder motion may provide damping to alleviate the buffeting of the fin by lagging accelerations by ninety degrees of phase. Therefore, the baseline control laws subtract phase at the frequencies of the first eigenmodes that the actuator phase lags fin tip accelerations by ninety degrees, Fig. 18b. The control laws consider also phase lags associated with the time delays caused by digital signal processing, especially by the digital controller, as well as the by actuator control unit. Consequently, the control law phase relations may be modified by a zero order hold to take these delays into account[22]. Avoiding excitation of higher frequency modes sufficient filtering is needed decreasing the control law gain beyond $k = 0.75$. Regarding the fin as a single degree–of–freedom system extensive dynamic simulations are conducted to prove the efficiency of the baseline control laws.[20] Stability gain margins are computed to ensure that the control law will not produce any instabilities.

5.2 Buffeting Reduction

The PSD results of the open–loop and closed–loop wind tunnel experiments demonstrate that with active auxiliary rudder control a substantial decrease of the fin tip accelerations referring to the first bending and torsion mode is achieved, Fig. 19. The commanded rudder motions reduce the corresponding PSD peak values by as much as 60% to 70%. This reduction in the structural response is obtained at gain factors well below the physical limits of the rudder driving system. Conducting these tests, a constant gain factor was used over the incidence range of interest. It is shown that with active control the structural dynamic loads are significantly lower indicating a decrease in the PSD peak value of at least 60% and a decrease in the rms value of at least 18%

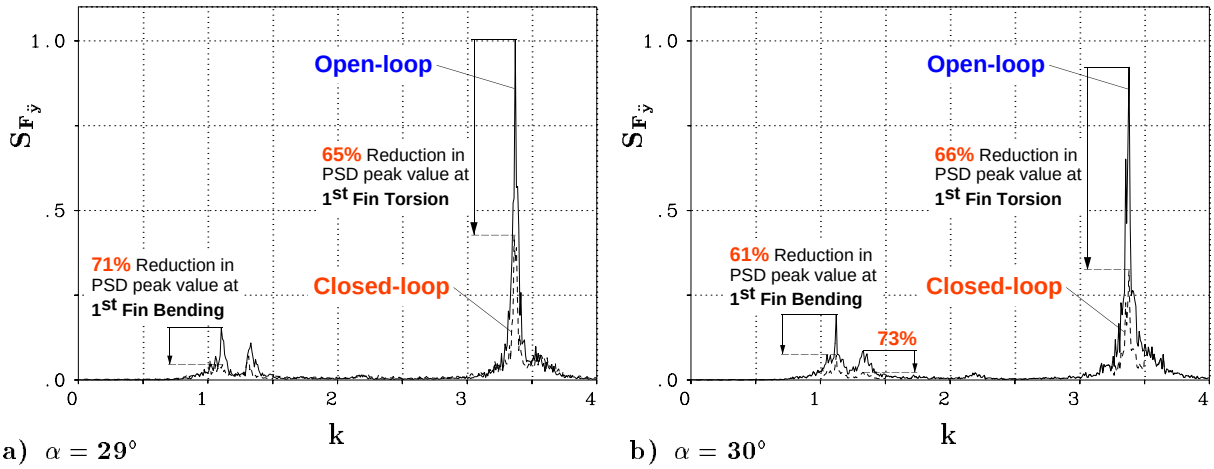

a) $\alpha = 29°$ b) $\alpha = 30°$

Fig. 19: Comparison of fin tip acceleration PSD's without and with active auxiliary rudder control at various angles of attack; $U_\infty = 40$ m/s, $Re_{l_\mu} = 0.97 \times 10^6$, $\beta = 0°$.

at all angles of attack investigated. Further improvement in the closed–loop response can be obtained by raising the gain factor in the control law within the stability region without driving the first fin bending or torsion mode, respectively, to increase the percentage of total damping added to the system by using active control.

5.3 Full–Scale Synthesis

The development of an active vibration alleviation system for the full–scale aircraft is strongly influenced by unsteady aerodynamics, flight mechanics and flight control, and aeroelastic effects. The relevant systems comprise the IMU to measure the induced vibrations, the flight control computers to implement the control laws, the comanded auxiliary rudder with its aeroelastic and aeroservoelastic properties and the aircraft itself which is affected in its flight mechanics and aeroelastic characteristics, Fig. 20. The feasibility of the auxiliary rudder concept and its performance has been also assessed in extensive theoretical analysis that involved the complete aircraft,[16,23] taking the small–scale results into account. The evaluation shows that buffeting may be reduced by approximately 50% in the first fin bending mode and by approximately 40% in the first fin torsion mode which is regarded to be quite promising (Fig. 20).

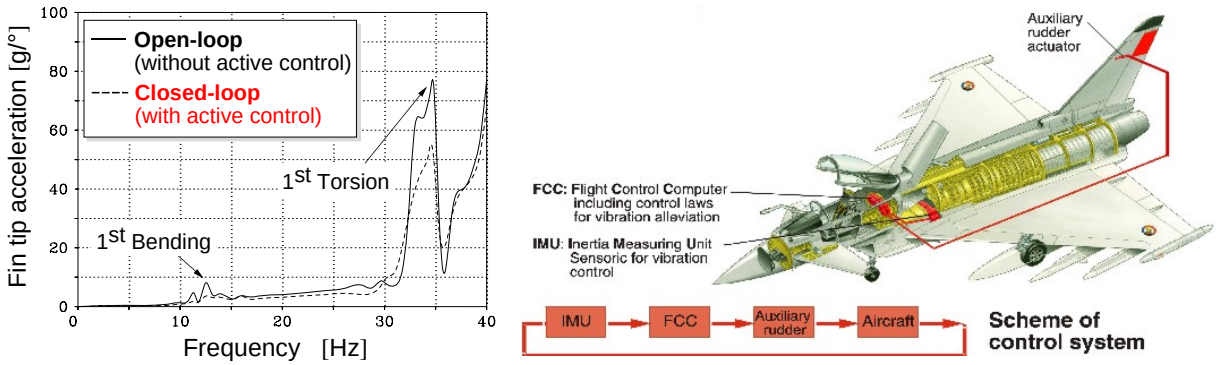

Fig. 20: Open–loop vs. closed–loop frequency response of fin lateral accelerations due to auxiliary rudder input simulated for a full–scale modern fighter aircraft (see Refs. 16, 23).

6 CONCLUSIONS AND OUTLOOK

Experimental investigations have been conducted on a modern fighter aircraft model to study aerodynamic active control in reducing single–fin buffeting. The focus is on the effectiveness of a commanded auxiliary rudder in altering buffet pressures and reducing vibrations in the first fin bending and torsion mode. A new fin model featuring an active auxiliary rudder has been fabricated and instrumented to measure unsteady surface pressures, fin tip accelerations and the transient rudder momemt. The auxiliary rudder oscillates harmonically with reduced frequencies of $k = 0$ to $k = 0.81$ driven by a digitally controlled servo motor via an excenter gear. The rudder efficiency is demonstrated by wind tunnel tests varying rudder frequency and maximum deflection angles at angles of attack up to 31 deg. The control laws are based on frequency domain compensation methods using measured open–loop frequency response functions to alleviate the buffeting of the fin.

These investigations show the following major results:

- For the oscillating auxiliary rudder, the fin surface pressure fluctuations increase with increasing rudder frequency and deflection angle. The corresponding rms values exhibit higher levels even at high angles of attack compared to the case with non–oscillating rudder. Closing the loop, the buffet pressures may be reduced by as much as 20 percent.

- The amplitude of the rudder moment remains nearly constant over the angle–of–attack range of interest while the phase angle takes on values of about $-20° \div -40°$. The constant

rudder moment substantiates the efficiency of the auxiliary rudder also in the high–α regime.

- Single–input single–output control laws are successfully employed to diminish vibrations (buffeting) in the first fin bending and torsion mode, respectively. A constant gain factor well below the physical limits of the rudder driving system gives satisfactory results at all angles of attack tested.
- The active control tests show that the peak values of the fin tip acceleration PSDs at the frequencies of the first bending and torsion mode can be reduced by as much as 60 percent for angles of attack up to 31 deg.
- Further improvements in buffeting alleviation may result from control law modifications to raise the control law gain factor within the stability region. Adaptive control methods using parameters depending on the angle of attack may also enhance the system performance in buffeting reduction.

7 ACKNOWLEDGMENT

This work was supported by the EADS GmbH (Military Aircraft Division). The author would like to thank Dr.-Ing. J. Becker (EADS–MT2) for a long period of fruitful cooperations.

8 REFERENCES

[1] Herbst, W. B., Future Fighter Technologies. *Journal of Aircraft*, Vol. 17, No. 8, 1980, pp. 561–566.

[2] Hummel, D., "*Documentation of Separated Flows for Computational Fluid Dynamics Validation*", AGARD–CP–437, Validation of Computational Fluid Dynamics, Vol. 2, Lisbon, Portugal, May 2-5, 1988, pp. 18-1–18-24.

[3] Breitsamter, C., "*Turbulente Strömungsstrukturen an Flugzeugkonfigurationen mit Vorderkantenwirbeln*", Dissertation, Technische Universität München, Herbert Utz Verlag, ISBN 3-89675-201-4, 1997.

[4] Luber, W., Becker, J., and Sensburg, O., "*The Impact Of Dynamic Loads On The Design of Military Aircraft*", AGARD–R–815, Loads and Requirements for Military Aircraft, Florence, Italy, Sept. 4-5, 1996, pp. 8-1–1-27.

[5] Colvin, B. J., Mullans, R. E., Paul, R. J., and Ross, H. N., "*F–15 Vertical Tail Vibration Investigations*", McDonnell–Douglas Corporation Report A6114, McDonnell Aircraft Company, St. Louis, MO, USA, Sept. 1979.

[6] Meyn, L. A., and James, K. D., "Full–Scale Wind Tunnel Studies of F/A–18 Tail Buffet", *Journal of Aircraft*, Vol. 33, No. 3, 1996, pp. 589–595.

[7] Lee, B. H. K., Brown, D., Zgela, M., and Poirel, D., "*Wind Tunnel Investigations and Flight Tests of Tail Buffet on the CF–18 Aircraft*", AGARD–CP–483, Aircraft Dynamic Loads due to Flow Separation, Sorrento, Italy, April 1-6, 1990, pp. 1-1–1-26.

[8] Del Frate, J. H., and Zuniga, F. A., "*In–Flight Flow Field Analysis On the NASA F–18 High Alpha Research Vehicle With Comparisons to Ground Facility Data*", AIAA Paper 90–0231, Jan. 1990.

[9] Rizk, Y. M., and Gee, K., "Unsteady Simulation of Viscous Flowfield Around F–18 Aircraft at Large Incidence", *Journal of Aircraft*, Vol. 29, No. 6, 1992, pp. 986–992.

[10] Ferman, M. A., Patel, S. R., Zimmermann, N. H., and Gerstenkorn, G., "*A Unified Approach to Buffet Response of Fighter Aircraft Empennage*", AGARD–CP–483, Aircraft Dynamic Loads due to Flow Separation, Sorrento, Italy, April 1-6, 1990, pp. 2-1–2-18.

[11] Breitsamter, C., and Laschka, B., "Fin Buffet Pressure Evaluation Based on Measured Flowfield Velocities", *Journal of Aircraft*, Vol. 35, No. 5, 1998, pp. 806–815.

[12] Breitsamter, C., and Laschka, B., "Turbulent Flow Structure Associated with Vortex–Induced Fin Buffeting", *Journal of Aircraft*, Vol. 31, No. 4, 1994, pp. 773–781.

[13] Breitsamter, C., and Laschka, B., "*Turbulent Flowfield Structure Associated to Fin Buffeting Around a Vortex–Dominated Aircraft Configuration at Sideslip*", Proceedings of the 19th Congress of the International Council of the Aeronautical Sciences, Vol. 1 (Paper No. ICAS–94–4.3.1), Anaheim, CA, USA, Sept. 18–23, 1994, pp. 768–784.

[14] Ferman, M. A., Liguore, S. L., Smith, C. M., and Colvin, B. J., "*Composite "Exoskin" Doubler Extends F–15 Vertical Tail Fatigue Life*", AIAA Paper 93–1341, 34th AIAA Structures, Structural Dynamics and Materials Conference, La Jolla, CA, USA, April 19-22, 1993.

[15] Ashley, H., Rock, S. M., Digumarthi, R. V., Chaney, K., and Eggers, Jr., A. J., "*Active Control for Fin Buffet Allevation*", Wright Laboratory Technical Report WL–TR–93–3099, Wright Patterson AFB, OH, USA, Jan. 1994.

[16] Becker, J., and Luber, W., "*Comparison of Piezoelectric and Aerodynamic Systems for Aircraft Vibration Alleviation*", SPIE 5th Annual Symposium on Smart Structures and Materials, Conf. Paper 3326–04, San Diego, CA, USA, March 1998.

[17] Hauch, R. M., Jacobs, J. H., Dima, C., and Ravindra, K., "Reduction of Vertical Tail Buffet Response Using Active Control", *Journal of Aircraft*, Vol. 33, No. 3, 1996, pp. 617–622.

[18] Moses, R. W., "*Vertical Tail Buffeting Alleviation Using Piezoelectric Actuators – Some Results of the Actively Controlled Response of Buffet–Affected Tails (ACROBAT) Program*", NASA–TM 110336, April 1997.

[19] Moses, R. W., "*Contributions To Active Buffeting Alleviation Programs By The NASA Langley Research Center*", AIAA Paper 99–1318, 40th AIAA/ASME/ ASCE/AHS/ASC Structures, Structural Dynamics, and Materials Conference, St. Louis, MO, USA, April 12-15, 1999.

[20] Breitsamter, C., and Laschka, B., "*Aerodynamic Active Control For EF–2000 Fin Buffet Load Alleviation*", AIAA Paper 2000-0656, 38th Aerospace Sciences Meeting & Exhibit, Reno, NV, USA, Jan. 10-13, 2000.

[21] Breitsamter, C., and Laschka, B., "*Fin Buffet Load Alleviation Using an Actively Controlled Auxiliary Rudder at Sideslip*", Proceedings of the 22nd Congress of the International Council of the Aeronautical Sciences (Paper No. ICAS–2000–3.10.2), Harrogate, UK, Aug. 27 - Sept. 1, 2000.

[22] Franklin, G. F., Powel, J. D., and Emami–Naeini, A., "*Feedback Control of Dynamic Systems*", Addison–Wesley Publishing Company, Reading, MA, 1986.

[23] Dürr, J. K., Herold-Schmidt, U., Zaglauer, H. W., and Becker, J., "*Active Fin–Buffeting Alleviation for Fighter Aircraft*", RTO/AVT Symposium On Active Control Technology For Enhanced Performance Operational Capabilities Of Military Aircraft, Land Vehicles And Sea Vehciles, Braunschweig, Germany, May 8-11, 2000.